





## Cycloartobiloxanthone, a Flavonoid with Antidiabetic, Antibacterial and Anticancer Activities from *Artocarpus kemando* Miq.

Tati Suhartati <sup>1\*</sup>, Antin S. Prihatin <sup>1</sup>, Armidla N. Kurniati <sup>1</sup>, Hendri Ropingi <sup>1</sup>,  
Yandri Yandri <sup>1</sup>, Sutopo Hadi <sup>1</sup>

<sup>1</sup> *Departement of Chemistry, Faculty of Mathematics and Natural Sciences, University of Lampung, Bandar Lampung 35145, Indonesia.*

### Abstract

In this present work, a cycloartobiloxanthone compound was isolated from the stem wood and root bark of the Pudau plant (*Artocarpus kemando* Miq.). The purity of the compound was determined using thin-layer chromatography with three eluent systems and melting point tests. The sample was then analyzed using UV-Vis, IR, and NMR spectroscopy, ensuring that the compound is cycloartobiloxanthone. The cycloartobiloxanthone compound was obtained in a yellow crystalline form with a melting point of 285.1-286.6 °C. The compound was then investigated for antidiabetic, anticancer, and antibacterial properties, showing that the compound has an anti-diabetic effect by reducing the activity of the  $\alpha$ -amylase enzyme, with the highest percentage of inhibition of  $48.53 \pm 1.84\%$  achieved with the use of 1000 ppm of the compound. Cycloartobiloxanthone isolated has an  $IC_{50}$  value of 9.21  $\mu$ g/mL for anticancer activity against MCF-7 cells, indicating that the compound shows active cytotoxic actions. *Staphylococcus aureus* was very strongly inhibited by the compound in the antibacterial test at all doses, whereas for *Salmonella* sp., the activity was categorized as moderate at concentrations of 0.4 and 0.3 mg/disc and strong at 0.5 mg/disc. The anti-diabetic, anti-cancer, and antibacterial bioactivity studies indicated that the cycloartobiloxanthone compound isolated has a broad spectrum of pharmacological actions, indicating that the compound has promising potential.

### Keywords:

Cycloartobiloxanthone;  
Antidiabetic;  
Anticancer;  
Antibacterial;  
*Artocarpus kemando* Miq.

### Article History:

Received:	19	September	2023
Revised:	27	December	2023
Accepted:	11	January	2024
Published:	01	February	2024

## 1- Introduction

Diabetes mellitus is a metabolic disease that causes hyperglycemia due to abnormalities in insulin production, insulin action, or both [1]. This disease is associated with genes or heredity, as well as the impact of poor living habits. According to the International Diabetes Federation [2], diabetes mellitus will affect 537 million individuals globally by 2021, with a predicted number of 643 million by 2030 and 783 million by 2045. In 2021, the costs required to handle diabetes reached around one trillion USD and will continue to increase if there are no breakthroughs in handling this chronic disease effectively and less costly. Currently, it is estimated that there are around 19.5 million people with diabetes in Indonesia, placing this country in fifth place among the countries with the most diabetes sufferers after China, India, Pakistan, and the United States. It is feared that this number will continue to increase and is likely to reach 45 million in 2045. In addition to the large number of sufferers, another disturbing fact is that diabetes sufferers are not limited to adults but also children and adolescents [3]. According to D'Souza et al. [4], diabetes cases in children and adolescents increased during the COVID-19 pandemic, reflecting the danger of diabetes as a severe chronic disease-causing complications and shortening life expectancy [5].

\* **CONTACT:** [tati.suhartati@fmipa.unila.ac.id](mailto:tati.suhartati@fmipa.unila.ac.id)

**DOI:** <http://dx.doi.org/10.28991/ESJ-2024-08-01-04>

© 2024 by the authors. Licensee ESJ, Italy. This is an open access article under the terms and conditions of the Creative Commons Attribution (CC-BY) license (<https://creativecommons.org/licenses/by/4.0/>).

Diabetes has a long-term impact that damages cells and tissues, resulting in a decrease in the immune system, which makes sufferers more susceptible to complications [6]. According to Ceriello & Prattichizzo [7], diabetic complications are caused by unstable glucose levels, blood pressure, plasma lipids, heartbeat, body weight, and serum uric acid. Cancer and bacterial infections are two examples of diabetic complications [8, 9]. According to Lega et al. [10], diabetics have a significantly greater risk of developing cancer than those without diabetes. The results of another study indicate that diabetic women have a greater mortality rate after breast cancer detection than non-diabetic women [11]. Furthermore, a weak body condition allows microbes from the environment, such as bacteria, to readily infiltrate the body, resulting in a variety of infections and diseases. High glucose levels allow germs to develop and disseminate more rapidly, making diabetics more susceptible to illness. According to Casqueiro et al. [12], diabetics suffer from infections in all organs and systems, including foot infections, invasive external otitis, rhinocerebral mucormycosis, and cholecystitis gangrene.

Up to present, the most widely used treatments for diabetes are insulin and several synthetic anti-diabetic drugs. According to Rai et al. [13], the use of insulin devices and pumps in diabetics has disadvantages such as the inability to mix different kinds of insulin, the need to keep the dosage low, skin irritation or hypersensitivity, and relatively high expense. Long-term use of synthetic medications is also problematic and therefore not recommended because this practice can lead to adverse effects. One common case is a leg infection caused by bacteria. To cure this infection, the most common practice is the use of antibiotics. Unfortunately, some bacteria are resistant to antibiotics, of which *Staphylococcus aureus*, *Escherichia coli*, and *Pseudomonas aeruginosa* are three examples that have been acknowledged as microorganisms [14–16].

In response to the antibiotic-resistance phenomenon, the search for alternative drugs has been focused on plant-derived anti-diabetic substances, in appreciation of their fewer or no adverse effects as well as being less expensive than synthetic drugs [17]. One class of plant-derived compound compounds that has been acknowledged to exhibit anti-diabetic effects is flavonoids. This class of compounds is also known to have a wide range of pharmacological effects, such as protecting the heart and nerves, preventing age-related neurodegenerative diseases, preventing Alzheimer's and stroke, reducing neuropathic pain, and having anticancer, antioxidant, anti-inflammatory, antimalarial, antiviral, antibacterial, and antifungal properties [18]. Flavonoids are secondary compounds found in different parts of plants and function not only as a constitutive agent but also as a defense system to protect plant tissues from microbial attack. Flavonoids are made up of 15 carbon atoms in their fundamental carbon structure. With the C6-C3-C6 configuration, these carbon atoms form two benzene rings and one propane chain [19].

Artocarpus plants are known to contain a variety of secondary metabolite substances with high bioactivity, such as flavonoids and their derivatives. In previous studies, various flavonoids have been isolated from the Puda (A. *kemando*), breadfruit (A. *altilis*), Kenangan (A. *rigida*), and jackfruit (A. *heterophyllus*) [20–23]. In previous works, successful isolations of several flavonoids from A. *kemando* Miq have been reported, such as prenylated flavone and xanthone [24, 25], artoindonesianin C, artomandin, artonol B, artosimmin [26], artonin E, artonin O, artobiloxanthone, and cycloartobiloxanthone from the bark of the plant [27].

In this study, flavonoids isolated from the stem wood and root bark of the Puda plant (A. *kemando* Miq.) were tested for anticancer, antibacterial, and antidiabetic activities. This study is supported by the finding of Suhartati et al., in which it was reported that the xanthoangelol isolated from A. *kemando* Miq. showed antibacterial properties against *Bacillus subtilis* as well as anticancer activities [28]. This investigation is also supported by the bioactivities of flavonoids from different plants reported by other workers. As an example, Lotulung et al. [29] reported that four flavonoid compounds isolated from the ethanol extract and ethyl acetate portion of the breadfruit plant (A. *altilis*) exhibit anti-diabetic activity. Hmidene et al. [30] discovered that O-methylated and glucuronosylated flavonoids obtained from *Tamarix gallica* could block the activity of the  $\alpha$ -glucosidase enzyme. Hesperetin, luteolin, quercetin, catechin, and rutin are flavonoid compounds that can block the activity of  $\alpha$ -amylase [31].

## 2- Material and Methods

### 2-1- Tools and Instrumentation

Glassware (Pyrex), micropipette (Eppendroff), autoclave (CV-EL 12L/18L Certoclave Sterilizer), oven (T60 Heracus), laminar air flow (CRUMA model 9005-FL), water bath (Memmert W 350), microscope, centrifuge, biosafety cabinet, multimode reader, and CO<sub>2</sub> incubator were used in this study. Melting point apparatus (MP-10 Stuart), Agilent Technologies FT-IR spectrophotometer, <sup>1</sup>H-NMR (Agilent DD2 system operating at 500 MHz) and <sup>13</sup>C-NMR (Agilent DD2 system operating at 125 MHz) spectrometers, and a spectrophotometer (Cary-100 UV-Vis from Agilent Technologies) were used for spectroscopic analyses.

### 2-2- Material

Samples of stem wood and root bark of the Puda plant (A. *kemando* Miq.) were obtained from Karang Anyar Hamlet, Klaten Village, Penengahan District, South Lampung. The solvents of *n*-hexane, methanol (CH<sub>3</sub>OH), and ethylacetate (EtOAc) used for extraction and chromatography are technical grade and distilled before use, but the solvents utilized for spectrophotometer analysis, which include methanol, were of proanalytical quality (p.a.). The anti-diabetic test material consists of *Bacillus* sp. type IIA  $\alpha$ -amylase enzyme (Sigma Aldrich), 95% acarbose (Sigma Aldrich), iodine (Merck), DMSO (Merck), HCl (Merck), and soluble starch (Sigma Aldrich). Cisplatin, antibiotics, dimethyl sulfoxide

(DMSO), phosphate buffered saline (PBS), PrestoBlue™ Cell Viability Reagent, Roswell Park Memorial Institute Medium (RPMI), fetal bovine serum (FBS), trypsin-EDTA, and trypan blue with pro-analytical quality are the MCF-7 cell cytotoxic test materials. The mixture of nutrient agar (Oxoid), methanol (Merck), amoxicillin, and ciprofloxacin was used as an antibacterial test material. *Salmonella* sp. and *S. aureus* were received from the Laboratory of Biochemistry at the University of Lampung.

### 2-3- Extraction and Isolation

The maceration method was applied for extraction, by soaking pudau stem wood powder (1.8 kg) in 4.8 L MeOH for 24 hours, which was repeated three times (a total of 3 days process). A rotary vacuum evaporator was used to concentrate the MeOH extract, yielding a mass of 50.53 g of crude extract. The non-polar fraction was separated by liquid-liquid extraction, and then n-hexane was added. A rotating vacuum evaporator was used to concentrate the MeOH extract (50.53 g, polar phase), which was then dissolved in acetone. Only 32.19 g of the extract was soluble in acetone, resulting in a gel-like substance. The acetone-soluble fraction was separated further using vacuum liquid chromatography in a silica column (10% n-hexane-EtOAc gradient), giving 37 fractions (Fr. 1A–10E). Due to the development of crystals adhering to the vial, Fr. 3C (276.1 mg) was chosen for further purification through silica gel column chromatography [ethyl acetate: n-hexane 15%, v/v], yielding two mixed fractions (Fr. 3C2 and Fr. 3C3). The 3C3 fraction was mixed with the 3C2 filtrate and refined further, yielding yellow crystals of the 3(C2)3b fraction (40 mg).

Pudau root bark powder (1.23 kg) was macerated in 4 L MeOH for 24 hours and was repeated three times (a total of 3 days process). A rotary vacuum evaporator was used to concentrate the MeOH extract, yielding a crude extract of 109.19 g. The non-polar fraction was separated using n-hexane, and the semipolar fraction was separated using ethyl acetate and subsequently concentrated using a rotary vacuum evaporator. The ethyl acetate fraction (53.34 g) was separated further using vacuum liquid chromatography in a silica column (10% n-hexane-EtOAc gradient), producing a total of 16 fractions (Fr. 1–16). Due to the development of crystals adhering to the vial, Fr. 10d (590 mg) was chosen for further purification through silica gel column chromatography [ethyl acetate: n-hexane 30%, v/v], yielding four combined fractions (Fr. 10d1, 10d2, 10d3, and 10dk). The 10d3 and 10dk fractions were mixed (10dm) and refined further, yielding yellow crystals (23 mg) of the 10dm2k fraction. The flow chart of the research can be seen in Figure 1.

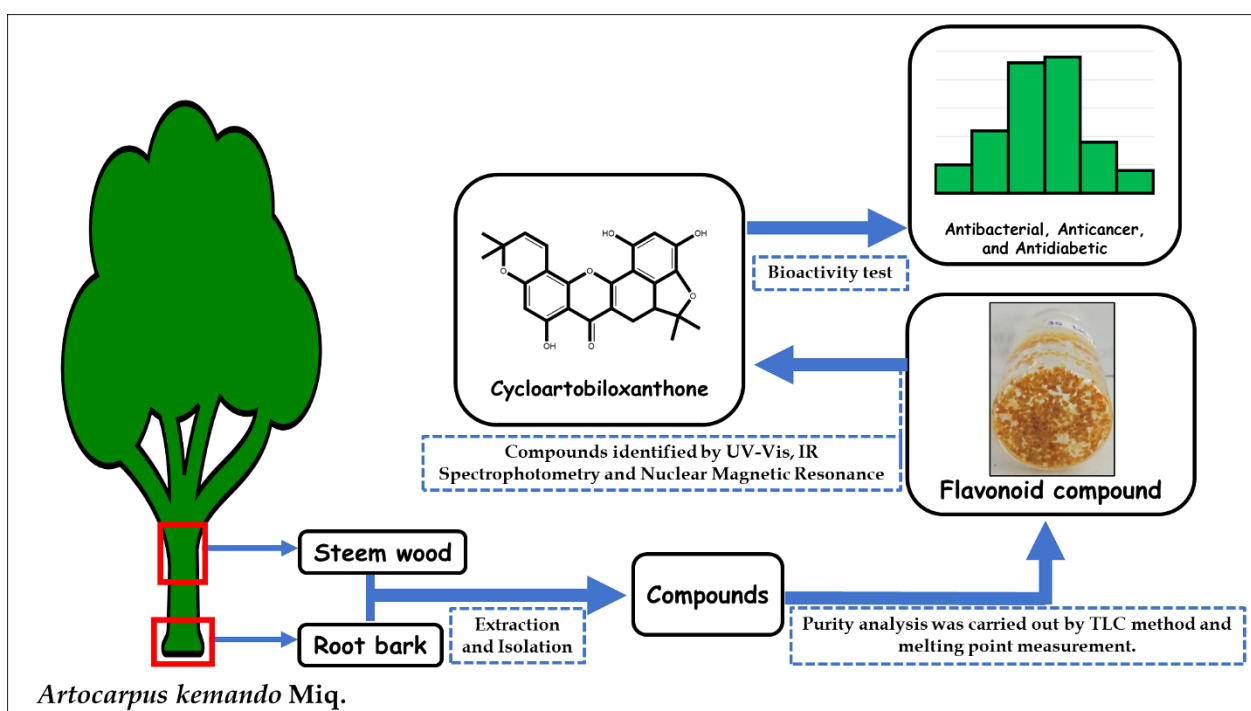


Figure 1. Flowchart of the research

### 2-4- Antidiabetic Test

The iodine test method was applied to determine the anti-diabetic bioactivity of the compounds [32], using starch as a substrate. In a test tube, 0.25 mL of inhibitor (flavonoid compounds) dissolved in DMSO was added to 0.25 mL of enzyme and incubated at room temperature for 10 minutes. After adding 0.25 mL of 1% starch solution, the mixture was incubated at 37°C for 30 minutes, with stirring every 10 minutes. By adding 0.25 mL of 1 N HCl, followed by 0.25 mL of iodine reagent, and 4 mL of distilled water, the reaction was stopped. After totally stirring the mixture, the absorbance of the sample at the maximum wavelength of 600 nm was measured using a UV-Vis spectrophotometer. As a comparison, measurements were also taken for acarbose. The following formula was used to calculate the activity of the sample, defined as the percentage of inhibition [33].

$$\text{Inhibition (\%)} = \left\{ 1 - \frac{(A2-A1)}{(A4-A3)} \times 100 \right\} \quad (1)$$

where A1 is absorbance of the solution containing sample, starch, and  $\alpha$ -amylase enzyme, A2 is absorbance of a solution containing sample and starch, A3 is absorbance of a solution containing starch and  $\alpha$ -amylase enzyme, and A4 is absorbance of solutions containing starch.

### 2-5-Anticancer Test

The anticancer test was performed by staining MCF-7 cells with PrestoBlue reagent according to the manufacturer's instructions. The cell culture was then cultured in 96 well plates at 37°C in a 5% CO<sub>2</sub> gas atmosphere until a percentage of cell growth of 70% was reached. The cells were cultured for 48 hours at 37°C in a 5% CO<sub>2</sub> gas atmosphere after being treated with the isolated compound and then treated with the presto blue working reagent. The absorbance of the sample at a wavelength of 570 nm was measured using a multimode reader. The anticancer test was carried out at the Central Laboratory of Padjadjaran University, Bandung, West Java.

### 2-6-Antibacterial Test

The paper disc method was used for the antibacterial test [34]. In 150 mL of distilled water, 4.2 grams of nutritional agar were dissolved and boiled for 15 minutes until the mixture turned into homogenous sample. The agar media were placed in test tubes containing up to 15 mL of agar media and up to 5 mL of distilled water per test tube. A petri dish was filled with 15 mL of agar medium per test tube. After the medium was ready, an aliquot of 5 mL of agar media that has been mixed with distilled water containing 1 loop of bacteria was placed in the medium. The compound isolated and the positive control were then prepared at three concentrations: 0.3, 0.4, and 0.5 mg/disk. A mass of 1.5 mg of sample was dissolved in 150  $\mu$ L methanol, then 30, 40, and 50  $\mu$ L of the solution were taken and stained onto disc paper. The paper discs holding samples, positive controls, and negative controls were then placed in the prepared medium. Positive controls in the antibacterial test used were amoxicillin for *S. aureus* and ciprofloxacin for *Salmonella* sp. The inhibitory zone was measured after the petri dish was covered with plastic wrap and placed in the incubator for 24 hours.

## 3- Results and Discussion

### 3-1-Purity Analysis

The purity of the crystals obtained from the isolation process was determined using melting point measurement and thin layer chromatography (TLC). The TLC method was used to confirm that the crystals obtained were pure and free of contaminants around the compound, with three variances in the resulting R<sub>f</sub> values. Based on the TLC chromatograms in the three eluent systems utilized, crystals from the wood section of the stem revealed a single stain, indicating the presence of Compound 1. The R<sub>f</sub> of the 10% MeOH: DCM eluent system was 0.71. The R<sub>f</sub> of the acetone: DCM 10% eluent system was 0.62. The R<sub>f</sub> of the 30% ethyl acetate: n-hexane eluent system was 0.22. While the crystals obtained from root bark displayed three distinct R<sub>f</sub> values in the three eluent systems studied, they were 0.22 in the ethyl acetate eluent variation: DCM (25%), 0.46 in the ethyl acetate eluent variation: n-hexane (50%), and 0.69 in the acetone eluent variation: n-hexane (80%). The three eluent systems all displayed a single spot on the TLC chromatogram; therefore, the compound was labeled as Compound 2.

Melting point measurements revealed that compound 1 has a melting point of 285.1–286.6 °C and compound 2 has a melting point of 292–294°C. Further analyses were then conducted using three different eluent systems to examine the stains and R<sub>f</sub> values of the two compounds. The three eluent systems used were DCM: ethyl acetate (25%), n-hexane: ethyl acetate (50%), and n-hexane: acetone (80%). The results of the TLC analysis are presented in Figure 2, indicating that the two samples displayed the same stains with the same R<sub>f</sub> values. Based on these TLC features, it is then concluded that the two samples are the same substance.

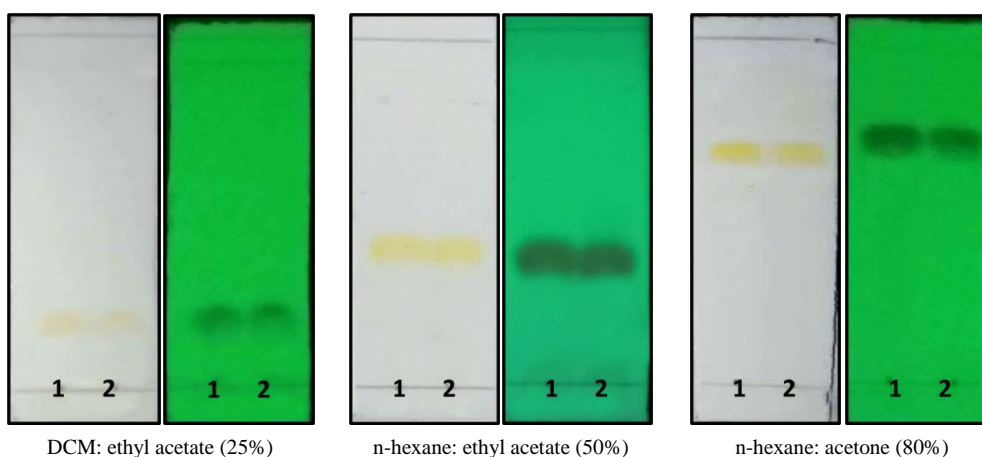
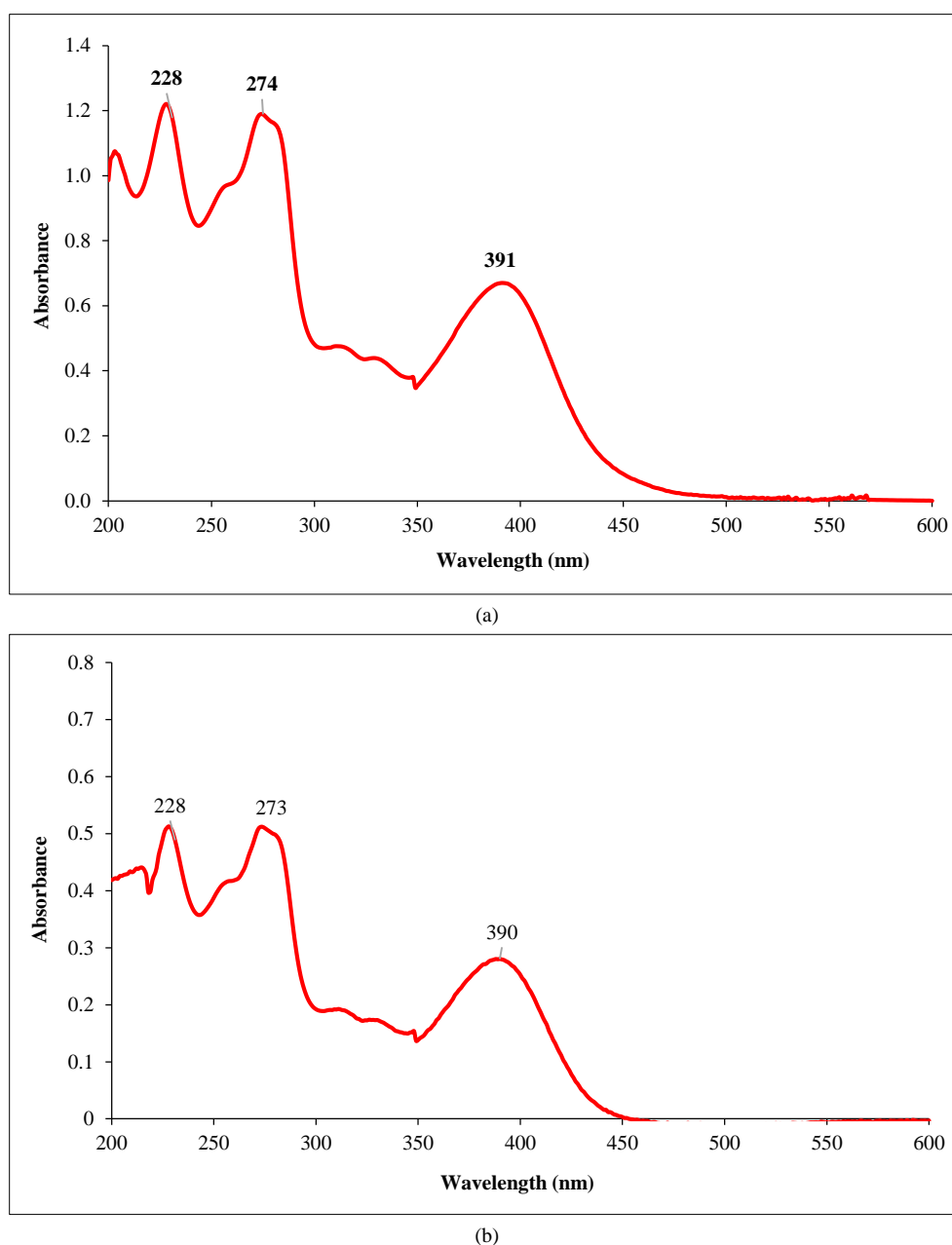


**Figure 2.** Comparison of TLC chromatograms of Compound 1 and 2

### 3-2-UV-Vis Spectroscopic Analysis

UV-Vis spectrophotometry analysis can be used to identify the types of flavonoids and their oxygenation patterns, determine the types of chromophores, conjugated double bonds, and auxochromes of organic compounds, and provide information about the structure of these compounds based on their wavelengths. As a general rule, flavonoid compounds are acknowledged to have a characteristic spectrum that consists of two bands, i.e., band I at 250–285 nm and band II at 300–550 nm [35].

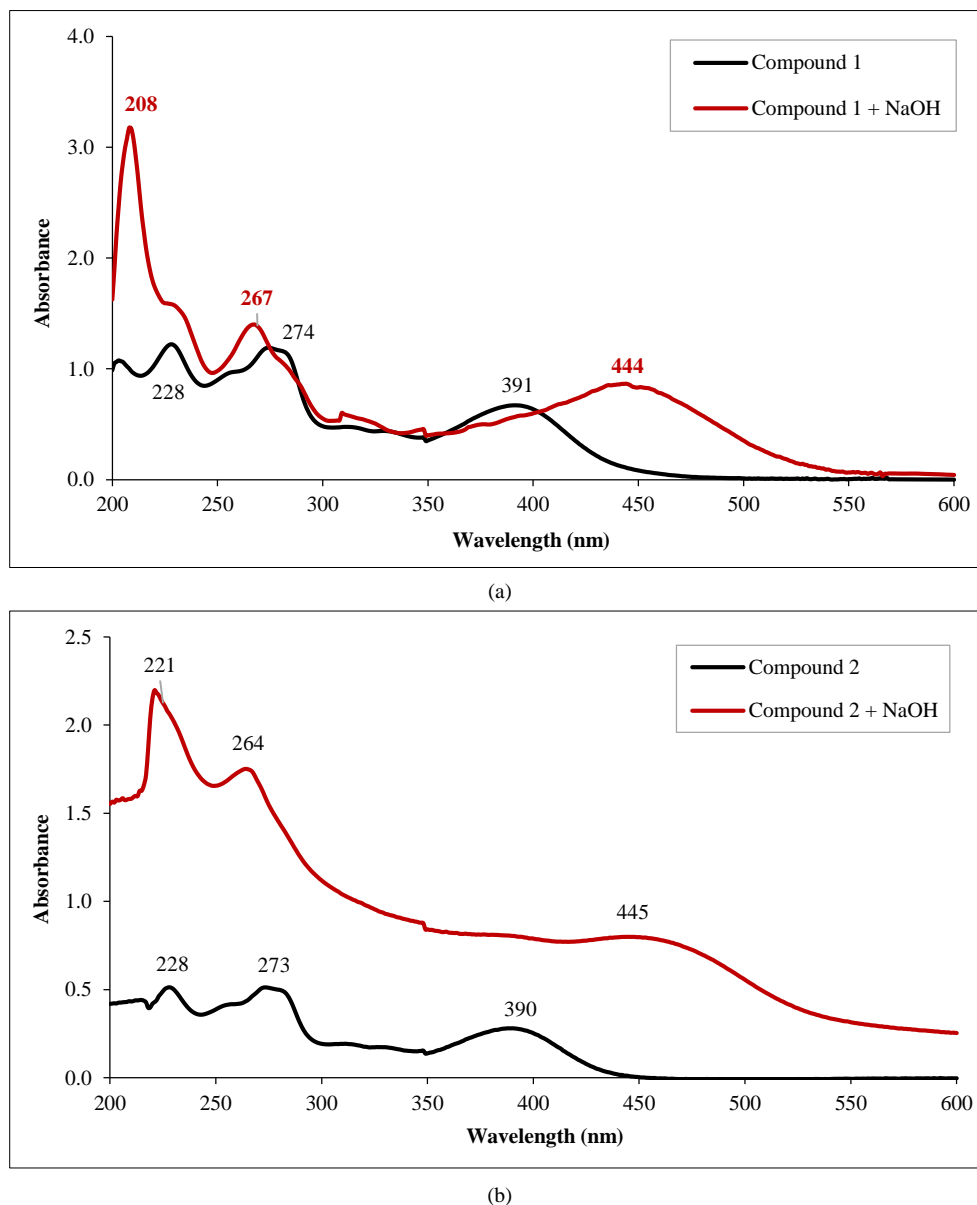
Figure 3 shows the UV-Vis spectrum of compound 1 and 2, displaying that compound 1 has three peaks with  $\lambda_{\max}$  of 228, 274 and 391 nm respectively, whereas compound 2 is characterized by the peaks at  $\lambda_{\max}$  of 228, 273, and 391 nm. In this respect, it can be seen that compounds 1 and 2 have comparable  $\lambda_{\max}$  values. The peaks at  $\lambda_{\max}$  of 390 and 391 nm in the band I of the spectrum of the compounds demonstrate the properties of flavone compounds for the cinnamoyl group resonance in ring B. The absorptions at  $\lambda_{\max}$  273 and 274 nm in band II are characteristic of a flavone spectrum, demonstrating the resonance of the benzoyl group in ring A. The peaks at  $\lambda_{\max}$  of 273 and 274 nm are associated with electron excitation from  $\pi \rightarrow \pi^*$ , which is a characteristic chromophore for an aromatic compound with conjugated double bond system ( $-\text{C}=\text{C}-\text{C}=\text{C}-$ ). The peaks at  $\lambda_{\max}$  of 390 and 391 nm reveal are associated with electron excitation from  $n \rightarrow \pi^*$ , indicating the presence of a heteroatom conjugated system with conjugated double bonds ( $-\text{C}=\text{C}-\text{C}=\text{O}$ ). Compounds 1 and 2 display a typical conjugated aromatic and carbonyl system for the flavonoid compound framework as revealed by the UV-Vis spectrum data [35].



**Figure 3.** UV-Vis Spectrum of (a) Compound 1 and (b) Compound 2

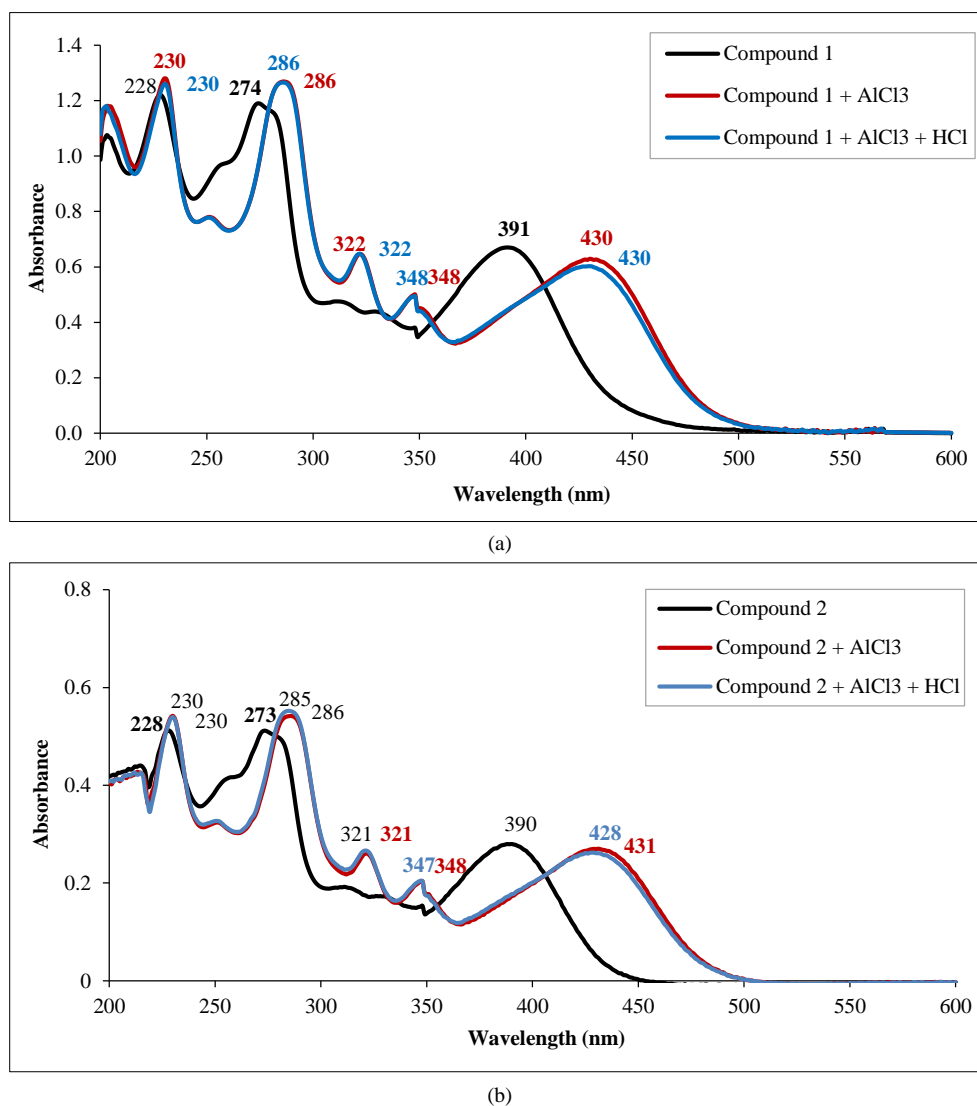


The location of the hydroxyl functional groups in the flavonoid core was established by examining the peak shift caused by the addition of a shear reagent. To detect more acidic and unsubstituted hydroxyl groups, NaOH shear reagent was added. The effects of NaOH shear reagent addition can be observed in the UV-Vis spectra shown in Figure 4. A 45-65 nm bathochromic shift in band I suggests the existence of a hydroxyl group at the C3' or C4' position. Because of the presence of particular substituents called auxochromes on the chromophore, the bathochromic effect causes a shift in absorbance from longer to shorter wavelengths. The addition of the NaOH shear reagent resulted in a bathochromic shift of 53 nm in band I for Compound 1 from  $\lambda_{\max}$  391 nm to 444 nm with increasing intensity, as shown in Figure 4A. Compound 2 exhibits a bathochromic shift of 55 nm in band I with increasing intensity, from  $\lambda_{\max}$  390 nm to 445 nm as can be observed in Figure 4B. The ionization of the base-sensitive hydroxyl groups causes this shift. The presence of a hydroxyl group at the C4' position is indicated by a bathochromic shift in band I accompanied by increased [26].



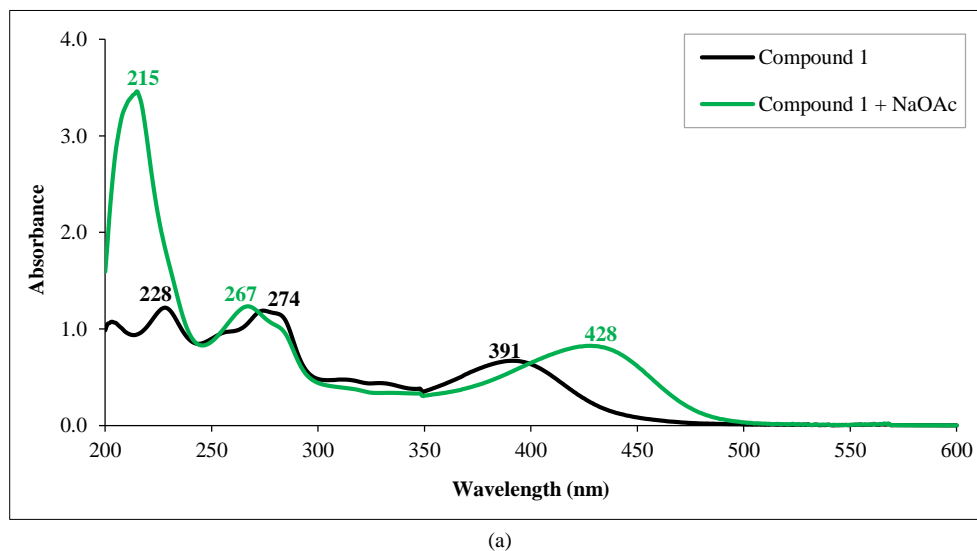
**Figure 4.** UV-Vis spectra of (a) Compound 1 and (b) Compound 2; before and after adding NaOH shift reagent

The shifting reagents  $\text{AlCl}_3$  and  $\text{AlCl}_3/\text{HCl}$  were used to identify the existence of a hydroxyl group near to ketone at the C5 position, as well as the presence of an ortho-dihydroxyl group in ring B. The results are compiled in Figure 5. Compound 1 had a bathochromic shift of up to 40 nm from  $\lambda_{\max}$  390 nm to 430 nm with increasing intensity in Figure 5A after adding the shift reagents  $\text{AlCl}_3$  and  $\text{AlCl}_3/\text{HCl}$  to the band I. Compound 2 likewise experienced a bathochromic shift in band I of 41 nm after the addition of  $\text{AlCl}_3$  shift reagent from  $\lambda_{\max}$  390 nm to 431 nm and a shift from 390 to 428 nm after adding  $\text{AlCl}_3/\text{HCl}$  shift reagent with increasing intensity in Figure 5B. The inclusion of the  $\text{AlCl}_3$  shear reaction causes a shift, indicating the existence of a hydroxyl group at the C5 position, near the ketone group. The change due to addition of  $\text{AlCl}_3/\text{HCl}$  addition suggests the existence of an ortho-dihydroxyl group in ring B. When  $\text{AlCl}_3/\text{HCl}$  was added, there is essentially little change in the absorption peak in band I, suggesting that the compound contains no ortho-dihydroxyl group in ring B [35].



**Figure 5.** UV-Vis spectra of (a) Compound 1 and (b) Compound 2; before and after adding AlCl<sub>3</sub>/HCl shift reagent

The occurrence of a bathochromic shift of 5-20 nm in band II, which is indicative of the presence of free 7-OH groups, was discovered using the NaOAc shift reagent, as demonstrated by the spectra in Figure 6. After the NaOAc shift reagent was added, the UV-Vis spectra in Figure 6 suggest the occurrence of a hypsochromic shift, which is shown as a shift in maximum absorbance to a lower wavelength in band II and a bathochromic shift in band I. Hypsochromic shifts of 7 nm from maximum 274 nm to 267 nm for compound 1 and 7 nm from maximum 273 nm to 266 nm for compound 2 in band II show the absence of a free hydroxyl group at the C7 position. Meanwhile, a reaction between the phenolic group in ring B and the NaOAc shear reagent results in the bathochromic shift in band I [35].



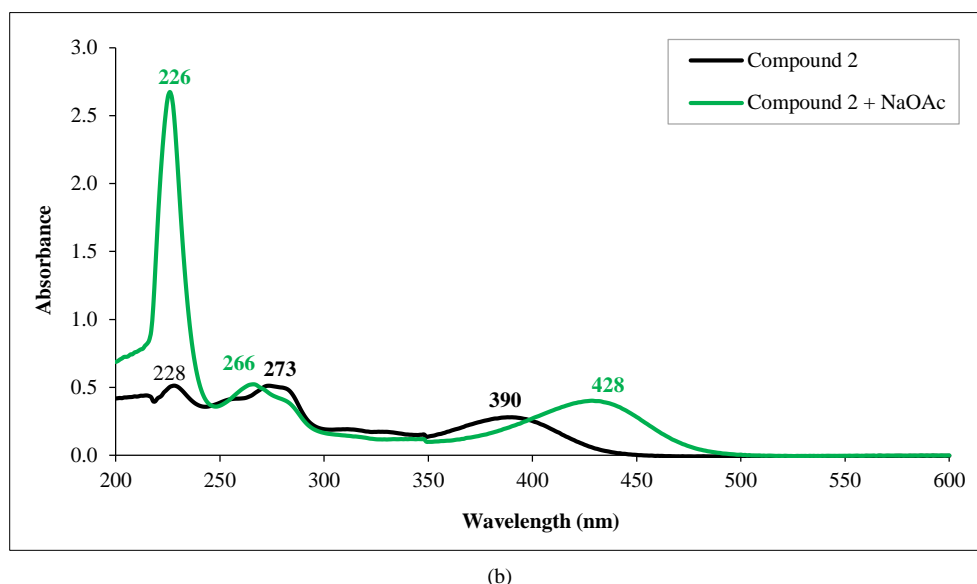


**Figure 6.** UV-Vis spectra of compound 1 (a) and compound 2 (b) before and after adding NaOAc shift reagent

The findings in Table 1 reveal that Compounds 1 and 2 have similar characteristics with cycloartobiloxanthone isolated from the plant *A. dadah* [36]. Because the isolated compounds contain the identical peaks at the UV-Vis wavelengths, it is assumed that Compounds 1 and 2 are cycloartobiloxanthone compounds. To confirm this assumption, further characterization was performed using an infrared spectrophotometer.

**Table 1.** Comparison of  $\lambda_{\max}$  UV-Vis spectra of cycloartobiloxanthone and isolated compounds after addition of shift

UV-Vis $\lambda_{\max}$ (nm)		
Compound 1	Compound 2	Cycloartobiloxanthone [36]
MeOH	MeOH	MeOH
391	390	390
274	273	274
228	228	228
MeOH+NaOH	MeOH+NaOH	MeOH+NaOH
444	445	435
267	264	265
208	221	229
MeOH+AlCl <sub>3</sub>	MeOH+AlCl <sub>3</sub>	MeOH+AlCl <sub>3</sub>
430	431	435
348	348	348
322	321	321
286	286	287
208	230	230
MeOH+AlCl <sub>3</sub> +HCl	MeOH+AlCl <sub>3</sub> +HCl	MeOH+AlCl <sub>3</sub> +HCl
430	428	435
348	347	348
322	321	321
286	285	287
230	230	230
MeOH+NaOAc	MeOH+NaOAc	MeOH+NaOAc
428	428	390
267	266	274
215	226	228



### 3-3-IR Spectroscopy Analysis

The presence of atomic vibrations in a molecule is the basis for this spectroscopic technique. Stretching, bending, and scissoring vibrations occur in the bonds between atoms as a result of interactions with the provided infrared waves. The absorbed IR wavelength corresponds to this vibrational frequency, which is unique and individual to each atomic bond. The IR wavenumbers vary from 625 to 4000  $\text{cm}^{-1}$ , in which the region at 625–1300  $\text{cm}^{-1}$  represents the fingerprint of each compound and demonstrates great specificity [37]. IR spectroscopy is mostly used to determine functional groups exist in the compounds [38]. Figure 7 depicts the IR spectra of Compounds 1 and 2 investigated.

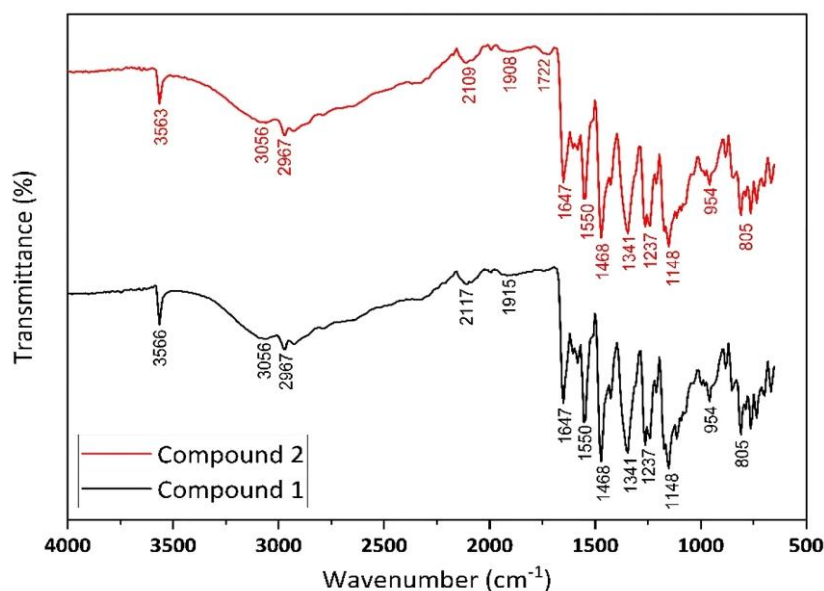


**Figure 7.** IR spectrum of Compounds 1 and 2 from the Pudau plant (*A. kemando* Miq.)

Compounds 1 and 2 have the same absorption peaks, according to data from an infrared spectrophotometer examination. Absorption peaks for compound 1 are located at wave numbers of 3566, 3056, 2967, 2117, 1915, 1647, 1550, 1468, 1341, 1237, and 1148  $\text{cm}^{-1}$ . The spectrum of compound 2 is marked by the presence of absorption peaks at wave numbers of 3563, 3056, 2967, 2109, 1908, 1722, 1647, 1550, 1468, 1341, 1237, and 1148  $\text{cm}^{-1}$ . Absorption in the wave numbers range of 3563–3566  $\text{cm}^{-1}$  reveals stretching vibrations emanating from the hydroxyl groups in phenol, which can form hydrogen bonds defined by tapering and sharp absorption bands. The presence of aliphatic C-H groups ( $\text{sp}^3$ ) is shown by absorption band at the wave number of 2967  $\text{cm}^{-1}$ . The existence of C-H vibrations in the aromatic rings is shown by the absorption peaks at wave numbers 1550–1468  $\text{cm}^{-1}$ , while the absorption band at 1647  $\text{cm}^{-1}$  confirms the existence of a carbonyl group conjugated with C=C. Table 2 compares the absorption peaks of the IR spectra of isolated compounds and typical cycloartobilosanthone compounds.

**Table 2.** Comparison of the absorption peaks of the IR spectra of Compounds 1 and 2 with standard cycloartobilosanthone compounds

Bonding Vibration ( $\text{cm}^{-1}$ )		
Compound 1	Compound 2	Cycloartobilosanthone [36]
3566	3563	3567
3056	3056	3117
2967	2967	2971
1647	1647	1654
1550	1550	1551
1468	1468	1476
1341	1341	1352
1237	1237	1265
1148	1148	1153
954	954	960
805	805	810

In the finger print region, the IR spectra of compounds 1 and 2 are characterized by absorption peaks at the same wave number ( $625\text{--}1300\text{ cm}^{-1}$ ). In this case, the best technique to assure an organic component is to compare its IR spectrum to that of its equivalent. Both samples indicate the same substance if their IR spectra in the fingerprint region match each other [39]. Other conventional cycloartobioxanthone compounds exhibit very identical absorption bands in the fingerprint areas of  $1352$ ,  $1265$ ,  $1153$ ,  $960$ , and  $810\text{ cm}^{-1}$  [36], suggesting that the two compounds are identical. Based on the results of characterizations of isolated compounds using UV-Vis and IR techniques as well as comparisons with standard compounds, it is then reasonable to conclude that the isolated compounds obtained from the stem wood (Compound 1) and root bark (Compound 2) of the Pudau plant (*A. kemando* Miq.) are cycloartobioxanthone compounds.

### 3-4- NMR Spectrometry Analysis

The compounds isolated were also characterized using Nuclear Magnetic Resonance technique, include  $^1\text{H}$ -NMR,  $^{13}\text{C}$ -NMR, HSQC,  $^1\text{H}$ - $^1\text{H}$  COSY, and HMBC. Figure 8 depicts the chemical shifts in the  $^1\text{H}$ -NMR spectrum of the isolated cycloartobioxanthone compound. The isolated cycloartobioxanthone compound's  $^1\text{H}$ -NMR spectrum reveals the presence of protons from  $\text{sp}^3$  carbon (methyl protons) at  $1.59\text{ ppm}$  (3H, s);  $1.44\text{ ppm}$  (3H, s);  $1.42\text{ ppm}$  (3H, s); and  $1.24\text{ ppm}$  (3H, s), which shows a singlet peak due to lack of coupling to other protons. Furthermore, the proton C  $\text{sp}^3$  at  $2.28\text{ ppm}$  (1H, t,  $J=15.3\text{ Hz}$ ) exhibits a triplet peak owing to proton coupling at  $3.11\text{ ppm}$ . The proton at  $3.11\text{ ppm}$  has a doublet (dd) peaks because it is connected to the proton at  $2.28\text{ ppm}$  (1H, t,  $J=15.3\text{ Hz}$ ).

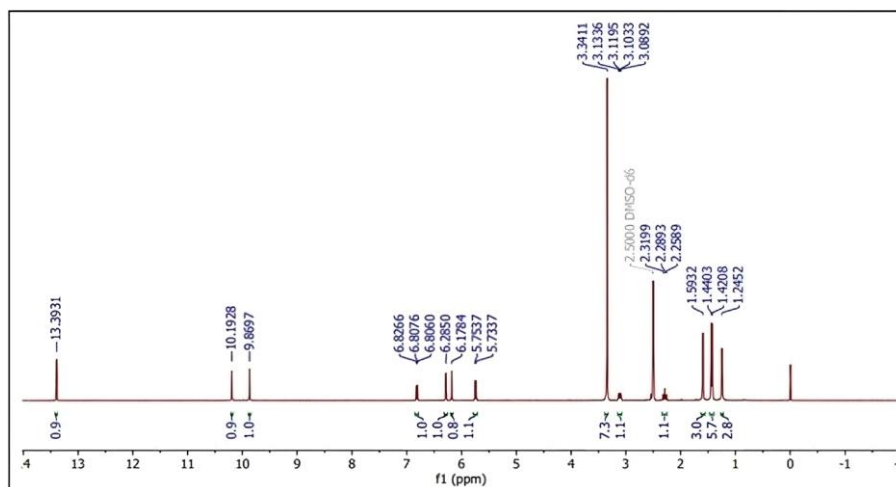


Figure 8. The  $^1\text{H}$ -NMR spectrum of the isolated cycloartobioxanthone compound

The spectrum indicates the presence of protons from the  $\text{sp}^3$  carbon as well as protons from the alkene chain  $\text{sp}^2$  carbon at  $6.81\text{ ppm}$  (1H, d,  $J=9.5\text{ Hz}$ ) and  $5.74\text{ ppm}$  (1H, d,  $J=10\text{ Hz}$ ), which are mutually exclusive and coupled to form a doublet peak in the spectrum. The proton of the aromatic ring's  $\text{sp}^2$  carbon was discovered at chemical shifts ( $\delta$ ) of  $6.28\text{ ppm}$  (1H, s) and  $6.17\text{ ppm}$  (1H, s), resulting in a singlet peak since it did not couple to other protons. The chemical shifts in Figure 8 are estimated to be:  $1.24\text{ ppm}$  (H-12);  $1.42\text{ ppm}$  (H-17);  $1.44\text{ ppm}$  (H-18);  $1.59\text{ ppm}$  (H-13);  $2.28\text{ ppm}$  (H-10);  $3.11\text{ ppm}$  (H-9);  $5.74\text{ ppm}$  (H-15);  $6.17\text{ ppm}$  (H-6);  $6.28\text{ ppm}$  (H-3');  $6.81\text{ ppm}$  (H-14);  $9.86\text{ ppm}$  ( $4'\text{OH}$ );  $10$ . The  $^{13}\text{C}$ -NMR spectrum, displayed in Figure 9, supports these  $^1\text{H}$ -NMR features.

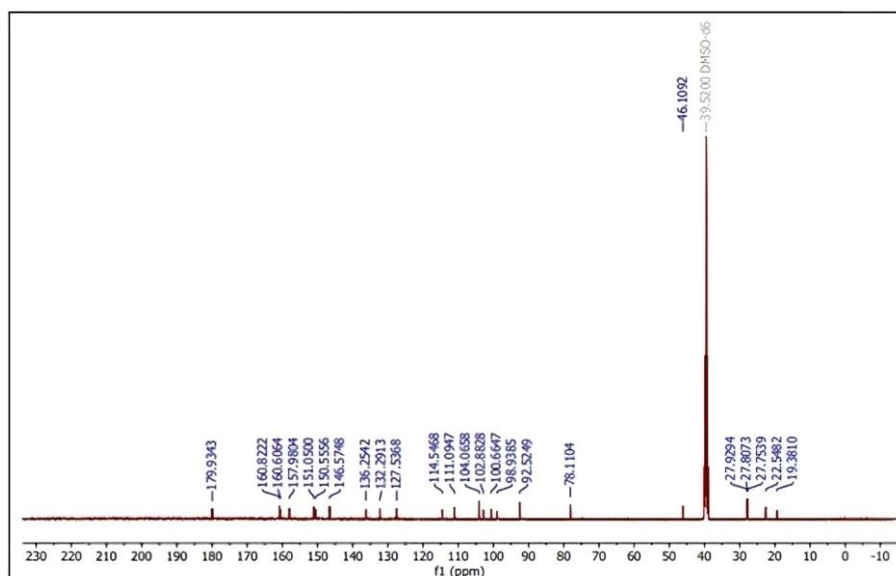


Figure 9. The  $^{13}\text{C}$ -NMR spectrum of the isolated cycloartobioxanthone compound

The  $^{13}\text{C}$ -NMR spectra revealed the existence of eight aromatic C atoms binding oxygen at 179.33 ppm (C-4), 160.82 ppm (C-2), 160.60 ppm (C-7), 157.98 ppm (C-8a), 151.05 ppm (C-5), 150.55 ppm (C-2'), 146.57 ppm (C-4'), and 136.25 ppm (C-5'). At 102.88 ppm (C-3') and 100.66 ppm (C-6), two aromatic C atoms bond to H atoms. Other aromatic C atoms may be observed at 111.09 ppm for C-1' and 98.93 ppm for C-8. The  $^1\text{H}$ -NMR and  $^{13}\text{C}$ -NMR spectra of the cycloartobiloxanthone compounds reported by Makmur et al. [40] are compared in Table 3.

**Table 3. Comparison of  $^1\text{H}$ -NMR and  $^{13}\text{C}$ -NMR spectrum data between the cycloartobiloxanthone and reference**

$^1\text{H}$ -NMR (ppm)		$^{13}\text{C}$ -NMR (ppm)		
Martinez-Gonzalez [31]	Cycloartobiloxanthone	C	Martinez-Gonzalez [31]	Cycloartobiloxanthone
1.35 (3H, s, H-12)	1.24 (3H, s, H-12)	2	160.8	160.82
1.47 (3H, s, H-17)	1.42 (3H, s, H-17)	3	103.6	-
1.48 (3H, s, H-18)	1.44 (3H, s, H-18)	4	180.6	179.93
1.58 (3H, s, H-13)	1.59 (3H, s, H-13)	4a	104.5	104.06
2.40 (1H, t, $J=15.1$ Hz, H-10)	2.28 (1H, t, $J=15.3$ Hz, H-10)	5	150.9	151.05
3.20 (2H, dd, $J=15.15$ & $7.05$ Hz, H-9a)	3.11 (2H, dd, $J=15.15$ & $7.05$ Hz, H-9a)	6	101.2	100.66
3.40 (2H, dd, $J=15.15$ & $7.05$ Hz, H-9b)	3.34 (2H, dd, $J=15.15$ & $7.05$ Hz, H-9b)	7	160.7	160.60
5.58 (1H, d, $J=10$ Hz, H-15)	5.74 (1H, d, $J=10$ Hz, H-15)	8	99.6	98.93
6.25 (1H, s, H-6)	6.17 (1H, s, H-6)	8a	158.6	157.98
6.25 (1H, s, H-3')	6.28 (1H, s, H-3')	9	19.5	19.38
6.85 (1H, d, H-14, $J=10.3$ Hz)	6.81 (1H, d, $J=9.5$ Hz, H-14)	10	46.4	46.10
	9.86 (4'-OH)	11	93.4	92.52
	10.19 (2'-OH)	12	22.3	22.54
	13.39 (5-OH)	13	27.7	27.75
		14	114.9	114.54
		15	127.0	127.53
		16	77.8	78.11
		17	27.7	27.80
		18	27.9	27.92
		1'	111.4	111.09
		2'	150.4	150.55
		3'	103.8	102.88
		4'	145.9	146.57
		5'	136.6	136.25
		6'	132.1	132.29

Table 3 demonstrates that the isolated cycloartobiloxanthone compound exhibits a proton chemical shift similar to the cycloartobiloxanthone compound reported by Makmur et al. [40]. HSQC (Heteronuclear Single Quantum Coherence) was used to examine the relationship/connectivity between the proton and the carbon linked to the isolated cycloartobiloxanthone compound. Using  $^1\text{H}$ - $^1\text{H}$  COSY, the relationship/connectivity between the protons and the protons bound to the isolated cycloartobiloxanthone compounds was investigated. Meanwhile, the long-distance correlation between protons and carbon was described in detail using the HMBC (Heteronuclear Multiple Bond Correlation) correlation spectrum. Table 4 shows the isolated cycloartobiloxanthone long distance connection and correlation between protons and carbon in more detail.

**Table 4. Long distance correlation data of isolated cycloartobiloxanthone compounds ( $\delta$  in ppm, J in Hz)**

Position	$\delta_{\text{H}}$	$\delta_{\text{C}}$	HMBC correlation
3'	6.28 (1H, s)	102.88	C-2', C-4', C-5'
6	6.17 (1H, s)	100.66	C-4a, C-5, C-7, C-8
9	3.11 (2H, dd, $J=15.15$ & $7.05$ )	19.38	C-3, C-6', C-9, C-11, C-12, C-13
10	2.28 (1H, t, $J=15.3$ )	46.10	C-2, C-3, C-4, C-6', C-10, C-11
12	1.24 (3H, s)	22.54	C-11
14	6.81 (1H, d, $J=9.5$ )	114.54	C-8, C-8a, C-15, C-16
15	5.74 (1H, d, $J=10$ )	127.53	C-8, C-16, C-17

Figure 10 shows a skeletal correlation of tricyclic flavonoids A-B-C based on long-distance correlation data (HMBC) from Table 4. The arrangement of protons and carbons in the isolated cycloartobiloxanthone structure conforms to the placement of protons and carbons in the cycloartobiloxanthone structure, as demonstrated by this correlation pattern.



Cycloartobiloxanthone and acarbose demonstrated the highest  $\alpha$ -amylase inhibitory action at 1000 ppm, with  $48.53 \pm 1.84\%$  and  $81.56 \pm 1.64\%$ , respectively. Figure 12 shows that the higher the concentration of both cycloartobiloxanthone and acarbose, the greater the percentage of inhibition achieved. Cycloartobiloxanthone, a flavonoid compound containing an active hydroxy group, functions as an enzyme inhibitor, lowering the effectiveness of the enzyme in the process. Flavonoid compounds that bind to enzymes alter the active site of the enzyme, making it harder to recognize by the substrate and interfering with the enzyme-substrate interaction. Nasution et al. (2015) [41] discovered that betasitosterol compounds derived from the bark of the *A. camansi* plant may decrease blood sugar levels in male Swiss Webster rats. Idris et al. (2022) [42] discovered that methanol extract from the leaves of the *Rhodomyrtus tomentosa* plant has antidiabetic effects of  $82.41 \pm 2.21\%$  against  $\alpha$ -amylase inhibition and  $81.91 \pm 1.09\%$  against  $\alpha$ -glucoamylase inhibition. Methanol extracts from the *Allium consanguineum* plant inhibited  $\alpha$ -amylase at concentrations of 62.5, 125, 250, 500, and 1000  $\mu\text{g/mL}$ , which was  $29.88 \pm 0.89\%$ ,  $42.78 \pm 0.45\%$ ,  $47.44 \pm 0.86\%$ ,  $64.72 \pm 0.89\%$ , and  $75.29 \pm 0.64\%$  [43].

The ability of flavonoid compounds to inhibit  $\alpha$ -amylase activity is the primary mechanism for their anti-diabetic effect. Cycloartobiloxanthone compounds reduce enzyme activity by attaching to the active site of the  $\alpha$ -amylase enzyme, inhibiting the enzyme's role in hydrolyzing starch to glucose as a consequence. The inhibitory impact is determined by two factors: (1) hydrogen bonding between the hydroxyl groups of the flavonoids at certain sites and the catalytic residue, and (2) the creation of conjugated systems within the flavonoids, which stabilize the connection with the active site. The conjugated system is generated on rings A and C by a C4 carbonyl group and a double bond C2, C3, as well as particular hydroxyl groups on C5 and C7 on ring A and C3' on ring B [44].

### 3-6-Anticancer Test

Using the PrestoBlue reagent, cycloartobiloxanthone isolated was tested for anticancer activity against MCF-7 breast cancer cells. The concentrations of cycloartobiloxanthone utilized were 3.91, 7.81, 15.63, 31.25, 62.50, 125.00, 250.00, and 500.00  $\mu\text{g/mL}$ . When living cells were added to the PrestoBlue reagent, the blue resazurin, which has no fluorescence phenomenon, changed to the highly fluorescent red product resorufin. After then, the absorbance was measured at 570 nm. The  $\text{IC}_{50}$  value of cycloartobiloxanthone in suppressing MCF-7 breast cancer cells is shown in Figure 13.

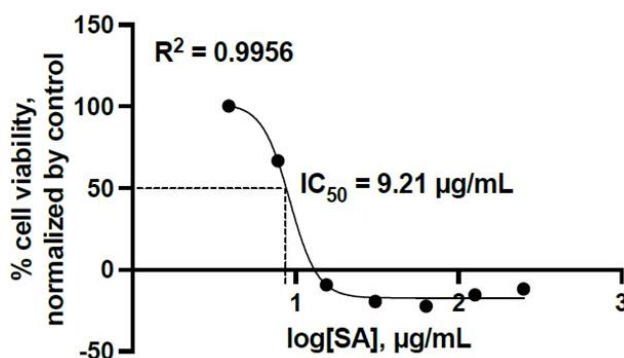


**Figure 13.** The results of the  $\text{IC}_{50}$  value of cycloartobiloxanthone compounds from *A. kemando* Miq. against MCF-7 cells

Based on  $\text{IC}_{50}$  values, Atjanasuppat et al. [45] divided cytotoxic activity into four groups: 20  $\mu\text{g/mL}$  active, > 20-100  $\mu\text{g/mL}$  moderate, >100-1000  $\mu\text{g/mL}$  weak, and >1000  $\mu\text{g/mL}$  inactive. Figure 13 depicts the anticancer impact of cycloartobiloxanthone on MCF-7 cells, with an  $\text{IC}_{50}$  value of 9.21  $\mu\text{g/mL}$  and active cytotoxic activity. Suhartati et al. [28] discovered that xanthoangelol compounds isolated from the leaves of *A. kemando* Miq. exhibited cytotoxic potential with active activity. In human lung cancer cells, cycloartobiloxanthone compounds produced from the stem bark of *A. gomezianus* show anticancer action [46]. Xanthohumol compounds, according to Jiang et al. [47], can act as anticancer agents against resistant MCF-7/ADR cells. Chethankumara et al. found that the methanol fractions of the stem bark and leaves of the *Alseodaphne semecarpifolia* plant have potential cytotoxicity against MCF-7 cells, with  $\text{IC}_{50}$  values of  $47.11 \pm 3.53 \mu\text{g/mL}$  and  $48.62 \pm 2.40 \mu\text{g/mL}$ , respectively [48]. Flavonoid compounds found in the plant *Eriocaulon cinereum* R.B. by phytochemical screening was reported to exhibit anticancer activity in MCF-7 cells with an  $\text{IC}_{50}$  of  $7.28 \pm 6.75 \mu\text{g/mL}$  [49]. According to Slika et al. [50], flavonoid compounds have anticancer properties because they are able to eliminate reactive oxygen species (ROS), inhibit oxidase enzyme, chelate metals, and activate antioxidant enzymes.

### 3-7-Antibacterial Test

After successfully isolating cycloartobiloxanthone from *A. kemando* Miq., antibacterial tests were performed against *S. aureus* and *Salmonella* sp. using the paper disc technique, with the width of the inhibition zone as indicator. According to Davis & Stout [51], hypothesis of antibacterial power, the strength of a compound based on antibacterial inhibitory



zone is classified into four categories: weak (5 mm), medium (5-10 mm), strong (10-20 mm), and very strong (>20 mm). In this investigation, three concentrations were employed in the antibacterial test: 0.3, 0.4, and 0.5 mg/disc. Amoxicillin was utilized as a positive control for *S. aureus* bacteria, whereas ciprofloxacin as a positive control for *Salmonella* sp. The results of antibacterial tests are displayed in Figures 14 and 15, while the widths of the sample inhibition zones are compiled in Tables 5 and 6.

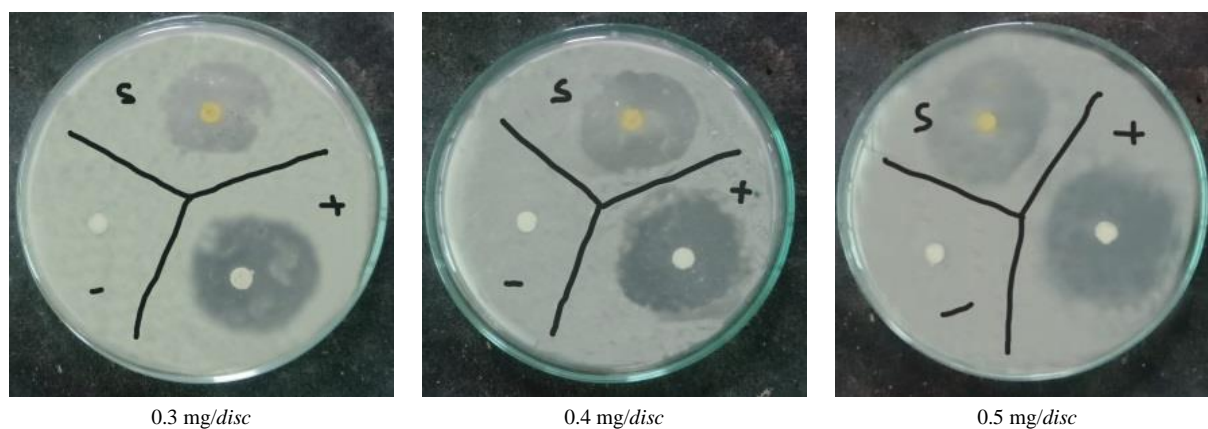


**Figure 14.** Antibacterial test results of cycloartobilosanthone compounds against *S. aureus* bacteria at various concentrations

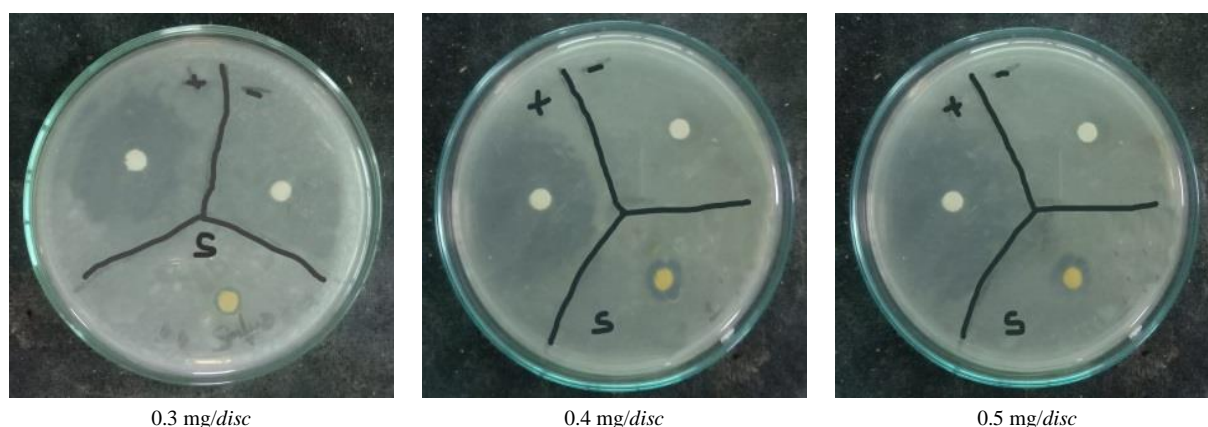


**Figure 15.** Antibacterial test results of cycloartobilosanthone compounds against *Salmonella* sp. bacteria at various concentrations

**Table 5.** The size of the inhibition zone of the cycloartobilosanthone antibacterial test against *S. Aureus*

Sample	Inhibition zone (mm)		
	Concentration		
	0.3 mg/disc	0.4 mg/disc	0.5 mg/disc
Cycloartobilosanthone	28	31	35
Control (+)	34	36	39
Control (-)	-	-	-

**Table 6.** The size of the inhibition zone of the cycloartobilosanthone antibacterial test against *Salmonella* sp

Sample	Inhibition zone (mm)		
	Concentration		
	0.3 mg/disc	0.4 mg/disc	0.5 mg/disc
Cycloartobilosanthone	8	10	13
Control (+)	39	42	47
Control (-)	-	-	-

Antibacterial bioactivity of cycloartobiloxanthone compounds against *S. aureus* bacteria was shown in Figure 14. At doses of 0.3, 0.4, and 0.5 mg/disc, cycloartobiloxanthone compounds had inhibitory zone widths of 28, 31, and 35 mm,



placing them in the very strong category. At the same concentration, the inhibition zone diameters of the amoxicillin positive control were 34, 36, and 39 mm, respectively. Suhartati et al. [28] discovered that xanthoangelol compounds isolated from the leaves of *A. kemando* Miq. displayed high antibacterial action against *B. subtilis*. Two compounds were identified: quercetin-3-O- $\alpha$ -L-(2''-E-p-coumaroyl-3''-Z-p-coumaroyl)-rhamnopyranoside (E,Z-30-hydroxyplatanoside) and quercetin-3-O- $\alpha$ -L-(2''-Z-p-coumaroyl-3''-E-p-coumaroyl)-rhamnopyranoside (Z,E-30-hydroxyplatanoside) from the leaves of the plant *Platanus acerifolia* showed significant inhibitory activity of *S. aureus* ATCC 25904 with MICs ranging between 4 to 64  $\mu$ g/mL [52]. According to Yu et al. [53] four analogues of the flavonoid type procyanidin B3-3-O-gallate (1), rhamnetin 3-O-(600-galloyl)- $\beta$ -D-glucopyranoside (2), rhamnetin 3-O- $\alpha$ -L-rhamnopyranoside (3), and quercetin 3-O-(600-galloyl)- $\beta$ -D-glucopyranoside (4) found in the methanol extract of *Woodfordia uniflora* leaves can inhibit *S. aureus* (strain USA300) with compounds 2 or 4 resulting in a significant reduction in MRSA biofilm formation.

The isolated cycloartobiloxanthone compound showed antibacterial bioactivity in the medium category, with inhibition zone diameters of 8 and 10 mm at concentrations of 0.3 and 0.4 mg/disc and specified as strong category, with inhibition zone diameters of 13 mm, at concentrations of 0.5 mg/disc. Ciprofloxacin was used as a positive control in this test because it has very strong antibacterial properties with an inhibition zone width of > 20 mm at doses of 0.3, 0.4, and 0.5 mg/disc. Suhartati et al. [28] discovered that the xanthoangelol compound isolated from the leaves of *A. kemando* Miq. Exhibited no antibacterial effect against *E. coli*. The dry ethanol extract of *Averrhoa bilimbi* L. leaf powder inhibited the growth of *Salmonella* sp. by  $27.00 \pm 1.73$  mm [54]. According to Abdallah et al. [55], ethyl acetate fraction extract from *Sclerocarya birrea* (A. Rich) stems may inhibit the growth of *Salmonella typhi*, with a maximum inhibitory zone at 10 mg/ml of  $9.7 \pm 0.0$  mm.

The results of antibacterial tests revealed that the cycloartobiloxanthone compound from the Puda plant (*A. kemando* Miq.) displayed inhibitory activity against *S. aureus* and *Salmonella* sp. The inhibitory zone revealed that the cycloartobiloxanthone compound exhibited stronger antibacterial activity against *S. aureus*, a Gram-positive bacteria, than against *Salmonella* sp., a Gram-negative bacteria. Gram-positive bacteria have a cell wall with a strong peptidoglycan content, minimal lipid, and polysaccharides (teichoic acid) but no outer membrane. The capacity of flavonoid compounds to establish complex interactions between proteins in the bacterial cell wall and the hydroxyl groups in flavonoid compounds gives them antibacterial bioactivity. According to Bouarab-Chibane et al. [56], flavonoids, which are phenolic compounds containing multiple -OH active groups, can be toxic to protoplasm, causing damage and penetration of the bacterial cell wall. The formation of hydrogen bonds between phenol groups and proteins causing a damage on the protein structure and reduces the permeability of the cell wall and cytoplasmic membrane.

## 4- Conclusion

The stem wood and root bark of the Puda plant (*A. kemando* Miq.) were successfully used to obtain pure flavonoid compounds with the same structure. UV-Vis spectrophotometry, IR spectroscopy, and NMR were used to validate the structure. The purity of the two flavonoid compounds was determined using the TLC method with three different eluent systems. The findings revealed that the two compounds were identical. The compound isolated from the stem wood and root bark has the structure of cycloartobiloxanthone. The compound was found to exhibit antidiabetic, anticancer, and antimicrobial properties. At a dosage of 1000 ppm, the compound demonstrated anti-diabetic characteristics by inhibiting the action of  $\alpha$ -amylase by  $48.53 \pm 1.84\%$ . In the active cytotoxic category, cycloartobiloxanthone has anticancer activity with an  $IC_{50}$  value of 9.21  $\mu$ g/mL against MCF-7 cells. This compound also demonstrated antimicrobial against *S. aureus* and *Salmonella* sp. According to these findings, the cycloartobiloxanthone from *A. kemando* Miq. has anti-diabetic, anti-cancer, and anti-bacterial bioactivity, showing that this flavonoid has a broad spectrum of pharmacological action, with promising potential to treat complicated diseases.

## 5- Declarations

### 5-1-Author Contributions

Conceptualization, T.S., Y.Y., and S.H.; methodology, T.S., A.S.P., A.N.K., H.R., Y.Y., and S.H.; software, H.R. and T.S.; validation, T.S., Y.Y., and S.H.; writing—original draft preparation, H.R.; writing—review and editing, T.S., Y.Y., and S.H.; visualization, H.R.; supervision, T.S. and Y.Y.; project administration, T.S., Y.Y., and S.H.; funding acquisition, T.S. All authors have read and agreed to the published version of the manuscript.

### 5-2-Data Availability Statement

The data presented in this study are available in the article.

### 5-3-Funding

The authors are grateful to the Ministry of Education, Culture, Research and Technology for funding this study based on Basic Research 2023 with contract numbers 027/E5/PG.02.00.PL/2023 on 12<sup>th</sup> April 2023 and 2192/UN26.21/PN/2023 on 17<sup>th</sup> April 2023.

#### 5-4- Acknowledgements

The authors acknowledged the Ministry of Education, Culture, Research, and Technology of Indonesia for assisting this study.

#### 5-5- Institutional Review Board Statement

Not applicable.

#### 5-6- Informed Consent Statement

Not applicable.

#### 5-7- Conflicts of Interest

The authors declare that there is no conflict of interest regarding the publication of this manuscript. In addition, the ethical issues, including plagiarism, informed consent, misconduct, data fabrication and/or falsification, double publication and/or submission, and redundancies have been completely observed by the authors.

### 6- References

- [1] Association, A. D. (2014). Diagnosis and classification of diabetes mellitus. *Diabetes Care*, 37(SUPPL.1), 81– 90. doi:10.2337/dc14-S081.
- [2] IDF. (2021). *IDF Diabetes Atlas 2021* (10<sup>th</sup> Ed.). International Diabetes Federation, Brussels, Belgium. Available online: [www.diabetesatlas.org](http://www.diabetesatlas.org) (accessed on March 2023).
- [3] Serbis, A., Giapros, V., Kotanidou, E. P., Galli-Tsinopoulou, A., & Siomou, E. (2021). Diagnosis, treatment and prevention of type 2 diabetes mellitus in children and adolescents. *World Journal of Diabetes*, 12(4), 344–365. doi:10.4239/wjd.v12.i4.344.
- [4] D’Souza, D., Empringham, J., Pechlivanoglou, P., Uleryk, E. M., Cohen, E., & Shulman, R. (2023). Incidence of Diabetes in Children and Adolescents During the COVID-19 Pandemic: A Systematic Review and Meta-Analysis. *JAMA Network Open*, 6(6), E2321281. doi:10.1001/jamanetworkopen.2023.21281.
- [5] Heald, A. H., Stedman, M., Davies, M., Livingston, M., Alshames, R., Lunt, M., Rayman, G., & Gadsby, R. (2020). Estimating life years lost to diabetes: outcomes from analysis of National Diabetes Audit and Office of National Statistics data. *Cardiovascular Endocrinology & Metabolism*, 9(4), 183–185. doi:10.1097/XCE.0000000000000210.
- [6] Tomic, D., Shaw, J. E., & Magliano, D. J. (2022). The burden and risks of emerging complications of diabetes mellitus. *Nature Reviews Endocrinology*, 18(9), 525–539. doi:10.1038/s41574-022-00690-7.
- [7] Ceriello, A., & Prattichizzo, F. (2021). Variability of risk factors and diabetes complications. *Cardiovascular Diabetology*, 20(1), 101. doi:10.1186/s12933-021-01289-4.
- [8] Yang, K., Liu, Z., Thong, M. S. Y., Doege, D., & Arndt, V. (2022). Higher Incidence of Diabetes in Cancer Patients Compared to Cancer-Free Population Controls: A Systematic Review and Meta-Analysis. *Cancers*, 14(7), 1808. doi:10.3390/cancers14071808.
- [9] Sjöholm, K., Carlsson, L. M. S., Svensson, P. A., Andersson-Assarsson, J. C., Kristensson, F., Jacobson, P., Peltonen, M., & Taube, M. (2022). Association of Bariatric Surgery with Cancer Incidence in Patients with Obesity and Diabetes: Long-term Results from the Swedish Obese Subjects Study. *Diabetes Care*, 45(2), 444–450. doi:10.2337/dc21-1335.
- [10] Lega, I. C., Wilton, A. S., Austin, P. C., Fischer, H. D., Johnson, J. A., & Lipscombe, L. L. (2016). The temporal relationship between diabetes and cancer: A population-based study. *Cancer*, 122(17), 2731–2738. doi:10.1002/cncr.30095.
- [11] Bronsveld, H. K., Jensen, V., Vahl, P., De Bruin, M. L., Cornelissen, S., Sanders, J., Auvinen, A., Haukka, J., Andersen, M., Vestergaard, P., & Schmidt, M. K. (2017). Diabetes and Breast Cancer Subtypes. *PLOS ONE*, 12(1), e0170084. doi:10.1371/journal.pone.0170084.
- [12] Casqueiro, J., Casqueiro, J., & Alves, C. (2012). Infections in patients with diabetes mellitus: A review of pathogenesis. *Indian Journal of Endocrinology and Metabolism*, 16(7), 27. doi:10.4103/2230-8210.94253.
- [13] Rai, I., Wanjari, A., & Acharya, S. (2021). Recent Advances in Insulin Delivery Devices and Modes of Insulin Therapy. *Journal of Pharmaceutical Research International*, 33(57B), 358–367. doi:10.9734/jpri/2021/v33i57b34067.
- [14] Abalkhail, A., & Elbehiry, A. (2022). Methicillin-Resistant *Staphylococcus aureus* in Diabetic Foot Infections: Protein Profiling, Virulence Determinants, and Antimicrobial Resistance. *Applied Sciences (Switzerland)*, 12(21), 10803. doi:10.3390/app122110803.
- [15] Lienard, A., Hosny, M., Jneid, J., Schuldiner, S., Cellier, N., Sotto, A., La Scola, B., Lavigne, J.-P., & Pantel, A. (2021). *Escherichia coli* Isolated from Diabetic Foot Osteomyelitis: Clonal Diversity, Resistance Profile, Virulence Potential, and Genome Adaptation. *Microorganisms*, 9(2), 380. doi:10.3390/microorganisms9020380.

- [16] Mohamed, W. F., Askora, A. A., Mahdy, M. M. H., EL-Hussieny, E. A., & Abu-Shady, H. M. (2022). Isolation and Characterization of Bacteriophages Active against *Pseudomonas aeruginosa* Strains Isolated from Diabetic Foot Infections. *Archives of Razi Institute*, 77(6), 2187–2200. doi:10.22092/ARI.2022.359032.2357.
- [17] Panigrahy, S. K., Bhatt, R., & Kumar, A. (2021). Targeting type II diabetes with plant terpenes: the new and promising antidiabetic therapeutics. *Biologia*, 76(1), 241–254. doi:10.2478/s11756-020-00575-y.
- [18] Ullah, A., Munir, S., Badshah, S. L., Khan, N., Ghani, L., Poulson, B. G., Emwas, A. H., & Jaremko, M. (2020). Important flavonoids and their role as a therapeutic agent. *Molecules*, 25(22), 5243. doi:10.3390/molecules25225243.
- [19] Santos, E. L., Maia, B. H. L. N. S., Ferriani, A. P., & Teixeira, S. D. (2017). *Flavonoids: Classification, Biosynthesis and Chemical Ecology. Flavonoids - From Biosynthesis to Human Health*, IntechOpen, London, United Kingdom. doi:10.5772/67861.
- [20] Suhartati, T., Fatimah, N., Yandri, Y., Kurniawan, R., Bahri, S., & Hadi, S. (2021). The anticancer, antimalarial, and antibacterial activities of moracalkon a isolated from *Artocarpus kemando* Miq. *Journal of Advanced Pharmacy Education and Research*, 11(4), 105–110. doi:10.51847/9NHxpCqzUD.
- [21] Suhartati, T., Epriyanti, E., Borisha, I., Yandri, Suwandi, J. F., Yuwono, S. D., Qudus, H. I., & Hadi, S. (2020). In vivo antimalarial test of artocarpin and in vitro antimalarial test of artonin M isolated from artocarpus. *Revista de Chimie*, 71(5), 400–408. doi:10.37358/RC.20.5.8150.
- [22] Suhartati, T., Hernawan, Suwandi, J. F., Yandri, & Hadi, S. (2018). Isolation of Artonin E From the Root Bark of *Artocarpus Rigida*, Synthesis of Artonin E Acetate and Evaluation of Anticancer Activity. *Macedonian Journal of Chemistry and Chemical Engineering*, 37(1), 35–42. doi:10.20450/mjcce.2018.1406.
- [23] Septama, A., Jantan, I., Panichayupakaranant, P., Aluwi, M. F. M., & Rahmi, E. (2020). Immunosuppressive and antibacterial activities of dihydromorin and norartocarpetin isolated from *Artocarpus heterophyllus* heartwoods. *Asian Pacific Journal of Tropical Biomedicine*, 10(8), 361. doi:10.4103/2221-1691.287162.
- [24] Hashim, N., Rahmani, M., Sukari, M. A., Ali, A. M., Alitheen, N. B., Go, R., & Ismail, H. B. M. (2010). Two new xanthenes from *Artocarpus obtusus*. *Journal of Asian Natural Products Research*, 12(2), 106–112. doi:10.1080/10286020903450411.
- [25] Shamaun, S. S., Rahmani, M., Hashim, N. M., Ismail, H. B. M., Sukari, M. A., Lian, G. E. C., & Go, R. (2010). Prenylated flavones from *Artocarpus altilis*. *Journal of Natural Medicines*, 64(4), 478–481. doi:10.1007/s11418-010-0427-4.
- [26] Ee, G. C. L., Teo, S. H., Rahmani, M., Lim, C. K., Lim, Y. M., & Go, R. (2011). Artomandin, a new xanthone from *Artocarpus kemando* (Moraceae). *Natural Product Research*, 25(10), 995–1003. doi:10.1080/14786419.2010.534471.
- [27] Seo, E. K., Lee, D., Young, G. S., Chai, H. B., Navarro, H. A., Kardono, L. B. S., Rahman, I., Cordell, G. A., Farnsworth, N. R., Pezzuto, J. M., Kinghorn, A. D., Wani, M. C., & Wall, M. E. (2003). Bioactive prenylated flavonoids from the stem bark of *Artocarpus kemando*. *Archives of Pharmacal Research*, 26(2), 124–127. doi:10.1007/bf02976656.
- [28] Suhartati, T., Andriyani, N., Yandri, Y., & Hadi, S. (2023). Xanthoangelol, geranilated chalcone compound, isolation from pudau leaves (*Artocarpus kemando* Miq.) as antibacterial and anticancer. *Physical Sciences Reviews*. doi:10.1515/psr-2022-0259.
- [29] Lotulung, P. D. N., Mozef, T., Risdian, C., & Darmawan, A. (2014). In vitro antidiabetic activities of extract and isolated flavonoid compounds from *Artocarpus altilis* (Parkinson) Fosberg. *Indonesian Journal of Chemistry*, 14(1), 7–11. doi:10.22146/ijc.21261.
- [30] Hmidene, A. Ben, Smaoui, A., Abdelly, C., Isoda, H., & Shigemori, H. (2017). Effect of O-methylated and glucuronosylated flavonoids from *Tamarix gallica* on  $\alpha$ -glucosidase inhibitory activity: Structure-activity relationship and synergistic potential. *Bioscience, Biotechnology and Biochemistry*, 81(3), 445–448. doi:10.1080/09168451.2016.1254538.
- [31] Martinez-Gonzalez, A. I., Díaz-Sánchez, G., de la Rosa, L. A., Bustos-Jaimes, I., & Alvarez-Parrilla, E. (2019). Inhibition of  $\alpha$ -amylase by flavonoids: Structure activity relationship (SAR). *Spectrochimica Acta - Part A: Molecular and Biomolecular Spectroscopy*, 206, 437–447. doi:10.1016/j.saa.2018.08.057.
- [32] Fuwa, H. (1954). A new method for microdetermination of amylase activity by the use of amylose as the substrate. *Journal of Biochemistry*, 41(5), 583–603. doi:10.1093/oxfordjournals.jbchem.a126476.
- [33] Mwakalukwa, R., Amen, Y., Nagata, M., & Shimizu, K. (2020). Postprandial hyperglycemia lowering effect of the isolated compounds from olive mill wastes - An inhibitory activity and kinetics studies on  $\alpha$ -glucosidase and  $\alpha$ -amylase enzymes. *ACS Omega*, 5(32), 20070–20079. doi:10.1021/acsomega.0c01622.
- [34] Bauer, A. W., Kirby, W. M., Sherris, J. C., & Turck, M. (1966). Antibiotic susceptibility testing by a standardized single disk method. *American Journal of Clinical Pathology*, 45(4), 493–496. doi:10.1093/ajcp/45.4\_ts.493.
- [35] Mabry, T., Markham, K. R., & Thomas, M. B. (2012). *The systematic identification of flavonoids*. Springer Science & Business Media, Berlin, Germany.

- [36] Suhartati, T. & Yandri, Y. (2007). Cycloartobilosanthone from stem bark and flavonoids in several parts of *Artocarpus dadah* which grows in Lampung. *Jurnal Sains MIPA*, 2(13), 82-86. (In Indonesian).
- [37] Sastrohamidjojo, H. (1991). *Chromatography*. Liberty, Yogyakarta, Indonesia.
- [38] Silverstein, R. W., & Bassler, G. C. (1962). Spectrometric identification of organic compounds. *Journal of Chemical Education*, 39(11), 546–553. doi:10.1021/ed039p546.
- [39] Yadav, L. D. S. (2005). *Organic Spectroscopy*. Springer Science Business Media, Berlin, Germany.
- [40] Makmur, L., Syamsurizal, S., Tukiran, T., Syamsu, Y., Achmad, S. A., Aimi, N., Hakim, E. H., Kitajima, M., Mujahidin, D., & Takayama, H. (1999). Artonol B and cycloartobioxanthone from the plant *Artocarpus teysmanii* MIQ. *Proceedings ITB*. 31(2), 63-68.
- [41] Nasution, R., Bahi, M., Saidi, N., & Junina, I. (2015, November).  $\beta$ -Sitosterol from Bark of *Artocarpus camansi* and its Antidiabetic Activity. *Proceedings of The Annual International Conference*, 9-11 September, 2015, Banda Aceh, Indonesian.
- [42] Idris, M., Sukandar, E. R., Purnomo, A. S., Martak, F., & Fatmawati, S. (2022). Antidiabetic, cytotoxic and antioxidant activities of *Rhodomyrtus tomentosa* leaf extracts. *RSC Advances*, 12(39), 25697–25710. doi:10.1039/d2ra03944c.
- [43] Mahnashi, M. H., Alqahtani, Y. S., Alqarni, A. O., Alyami, B. A., Alqahtani, O. S., Jan, M. S., Hussain, F., Islam, Z. U., Ullah, F., Ayaz, M., Abbas, M., Rashid, U., & Sadiq, A. (2022). Phytochemistry, anti-diabetic and antioxidant potentials of *Allium consanguineum* Kunth. *BMC Complementary Medicine and Therapies*, 22(1), 154. doi:10.1186/s12906-022-03639-5.
- [44] Takahama, U., & Hirota, S. (2018). Interactions of flavonoids with  $\alpha$ -amylase and starch slowing down its digestion. *Food & Function*, 9(2), 677–687. doi:10.1039/c7fo01539a.
- [45] Atjanasuppat, K., Wongkham, W., Meepowpan, P., Kittakoop, P., Sobhon, P., Bartlett, A., & Whitfield, P. J. (2009). In vitro screening for anthelmintic and antitumour activity of ethnomedicinal plants from Thailand. *Journal of Ethnopharmacology*, 123(3), 475–482. doi:10.1016/j.jep.2009.03.010.
- [46] Losuwannarak, N., Sritularak, B., & Chanvorachote, P. (2018). Cycloartobioxanthone induces human lung cancer cell apoptosis via mitochondria-dependent apoptotic pathway. *In Vivo*, 32(1), 71–78. doi:10.21873/in vivo.11206.
- [47] Jiang, C. H., Sun, T. L., Xiang, D. X., Wei, S. S., & Li, W. Q. (2018). Anticancer activity and mechanism of xanthohumol: A prenylated flavonoid from hops (*Humulus lupulus* L.). *Frontiers in Pharmacology*, 9. doi:10.3389/fphar.2018.00530.
- [48] Chethankumara, G. P., Nagaraj, K., & Krishna, V. (2021). In vitro cytotoxic potential of alkaloid and flavonoid rich fractions of *alseodaphne semecarpifolia* against MCF-7 cells. *Biomedical and Pharmacology Journal*, 14(2), 557–565. doi:10.13005/bpj/2158.
- [49] Nugraha, A. T., Ramadani, A. P., Werdyani, S., Pratiwi, I. A., Juniardy, T., Arfadila, S., & Mahardhika, M. R. P. (2021). Cytotoxic activity of flavonoid from local plant *Eriocaulon cinereum* R.B against MCF-7 breast cancer cells. *Journal of Advanced Pharmaceutical Technology & Research*, 12(4), 425–429. doi:10.4103/japtr.japtr\_69\_21.
- [50] Slika, H., Mansour, H., Wehbe, N., Nasser, S. A., Iratni, R., Nasrallah, G., Shaito, A., Ghaddar, T., Kobeissy, F., & Eid, A. H. (2022). Therapeutic potential of flavonoids in cancer: ROS-mediated mechanisms. *Biomedicine & Pharmacotherapy*, 146, 112442. doi:10.1016/j.biopha.2021.112442.
- [51] Davis, W. W., & Stout, T. R. (1971). Disc Plate Method of Microbiological Antibiotic Assay. *Applied Microbiology*, 22(4), 659–665. doi:10.1128/am.22.4.659-665.1971.
- [52] Wu, X., Tang, Y., Osman, E. E. A., Wan, J., Jiang, W., Yang, G., Xiong, J., Zhu, Q., & Hu, J. F. (2022). Bioassay-Guided Isolation of New Flavonoid Glycosides from *Platanus × acerifolia* Leaves and Their *Staphylococcus aureus* Inhibitory Effects. *Molecules*, 27(17), 5357. doi:10.3390/molecules27175357.
- [53] Yu, J. S., Kim, J. H., Rashan, L., Kim, I., Lee, W., & Kim, K. H. (2021). Potential Antimicrobial Activity of Galloyl-Flavonoid Glycosides from *Woodfordia uniflora* Against Methicillin-Resistant *Staphylococcus aureus*. *Frontiers in Microbiology*, 12, 784504. doi:10.3389/fmicb.2021.784504.
- [54] Iwansyah, A. C., Desnilasari, D., Agustina, W., Pramesti, D., Indriati, A., Mayasti, N. K. I., Andriana, Y., & Kormin, F. B. (2021). Evaluation on the physicochemical properties and mineral contents of *averrhoa bilimbi* L. Leaves dried extract and its antioxidant and antibacterial capacities. *Food Science and Technology (Brazil)*, 41(4), 987–992. doi:10.1590/fst.15420.
- [55] Abdallah, M. S., Mustafa, M., Nallappan, M. A., Choi, S., Paik, J. H., & Rusea, G. (2021). Determination of Phenolics and Flavonoids of Some Useful Medicinal Plants and Bioassay-Guided Fractionation Substances of *Sclerocarya birrea* (A. Rich) Hochst Stem (Bark) Extract and Their Efficacy Against *Salmonella typhi*. *Frontiers in Chemistry*, 9, 670530. doi:10.3389/fchem.2021.670530.
- [56] Bouarab-Chibane, L., Forquet, V., Lantéri, P., Clément, Y., Léonard-Akkari, L., Oulahal, N., Degraeve, P., & Bordes, C. (2019). Antibacterial properties of polyphenols: Characterization and QSAR (Quantitative structure-activity relationship) models. *Frontiers in Microbiology*, 10. doi:10.3389/fmicb.2019.00829.